

## Theoretical and Experimental Study of the Regioselectivity of Michael Additions

David C. Chatfield,<sup>\*[a]</sup> Alberto Augsten,<sup>[a]</sup> Cassian D' Cunha,<sup>[a]</sup> Elzbieta Lewandowska,<sup>[b]</sup> and Stanislaw F. Wnuk<sup>[a]</sup>

**Keywords:** Density functional calculations / Michael addition / Regioselectivity / Substituent effects / Transition states

Nucleophilic attack at an  $\alpha,\beta$ -unsaturated carbonyl moiety usually results in conjugate addition at the  $\beta$ -carbon atom (1,4 or Michael addition) or, occasionally, in addition at the carbonyl carbon atom (1,2 addition). Recently, however, addition at the  $\alpha$ -carbon atom has been observed when strongly electron-withdrawing groups are positioned at the carbon atom  $\beta$  relative to the carbonyl group [e.g., methyl 3,3-bis(trifluoromethyl)propenoate (**8**) and ethyl 3-(2,4-dinitrophenyl)propenoate (**24**)]. We have performed theoretical calculations [HF/6-31+G(d) and B3LYP//HF/6-31+G(d)] for the addition of cyanide anion to model  $\alpha,\beta$ -unsaturated carbonyl compounds to determine trends in the regioselectivity with

respect to properties of the substituents. The difference between the reaction barriers for  $\alpha$ - vs.  $\beta$ -addition decreases as the strength of electron-withdrawing groups increases until, for sufficiently strong electron-withdrawing groups,  $\alpha$ -addition becomes favored. The calculations are in agreement with the experimental results. We show that the regioselectivity can be predicted from partial atomic charges and properties of the frontier orbitals of the reactants. We also report new experimental evidence of  $\alpha$ -addition to polysubstituted cinnamates and cinnamaldehydes.

© Wiley-VCH Verlag GmbH & Co. KGaA, 69451 Weinheim, Germany, 2004)

### Introduction

Nucleophilic addition to an  $\alpha,\beta$ -conjugated carbonyl moiety is among the most useful organic reactions and has a long history of study and use. Most often addition is at  $C_\beta$ , in a reaction termed Michael, conjugate, or 1,4 addition.<sup>[1]</sup> In some circumstances, addition at the carbonyl carbon atom occurs, i.e., 1,2 addition. Both of these processes have been studied theoretically<sup>[2–10]</sup> as well as experimentally.<sup>[1]</sup> The regioselectivity has been shown to be under frontier control<sup>[11,12]</sup> in the former case and under charge control in the latter.<sup>[2]</sup> Recently, reverse addition of nucleophiles (at  $C_\alpha$ ) to  $\alpha,\beta$ -unsaturated carbonyl compounds possessing strongly electron-withdrawing groups (EWGs) at  $C_\beta$  has been reported.<sup>[13,14]</sup> This process can be understood as a competition between EWGs on either side of the activated double bond. For example, reactions of dimethylamine or methanol with methyl 3,3-bis(trifluoromethyl)propenoate (**8**) give the corresponding  $\alpha$ -adducts,<sup>[13]</sup> as do additions of thiols to 2,4-dinitro- (e.g., **24**) and 2,4,6-trinitrocinnamates.<sup>[14]</sup> Phosphane-catalyzed reaction of nitrogen nucleophiles with 2-alkynoates redirects the regioselectivity of ad-

dition of a nucleophile from the classical  $\beta$ -addition to an  $\alpha$ -addition mode.<sup>[15]</sup> We refer to reactions such as these as  $\alpha$ -additions.

In this article, we report theoretical calculations on reactants, transition states, intermediates, and products for  $\alpha$ - and  $\beta$ -addition to a series of model compounds. We also report new experimental evidence for  $\alpha$ -additions that is in agreement with the results of calculations. Our purposes are to predict when  $\alpha$ -addition will occur, to determine whether the reported cases of  $\alpha$ -addition reflect regular trends with respect to properties of substituents attached to  $C_\beta$ , and to determine factors controlling the regioselectivity.

### Research Design and Assumptions

**Calculations:** We investigated the effect of the EWGs F,  $CF_3$ , CHO, and  $NO_2$  on the energies of transition states and intermediates for  $\alpha$ - and  $\beta$ -addition. The EWGs were positioned either directly on  $C_\beta$  or on a vinyl group or a phenyl ring attached to  $C_\beta$ . The list of compounds studied is given in Table 1. The models were chosen to assess methodically the influence of separation between the electron-withdrawing group and  $C_\beta$ . Compounds **1–10** are propenals and methyl propenoates, **11–16** are pentadienals and methyl pentadienoates, and **17–22** are cinnamaldehydes.

We expect the nucleophilic addition step to be rate-determining. Therefore, we calculated the conformations and energies of the transition states dividing reactants from in-

<sup>[a]</sup> Departments of Chemistry, Florida International University  
Miami, Florida 33199, USA  
Fax: (internat.) + 1-305-348-3772  
E-mail: David.Chatfield@fiu.edu

<sup>[b]</sup> University of Agriculture  
60-625 Poznan, Poland

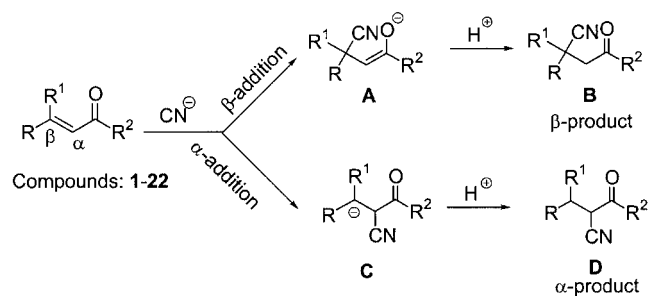
Supporting information for this article is available on the WWW under <http://www.eurjoc.org> or from the author.

Table 1. Differences (kcal/mol) between energies<sup>a</sup> of transition states ( $\Delta E^{\text{TS}} = E_{\alpha}^{\text{TS}} - E_{\beta}^{\text{TS}}$ ), intermediates ( $\Delta E^{\text{I}} = E_{\alpha}^{\text{I}} - E_{\beta}^{\text{I}}$ ), and products ( $\Delta E^{\text{P}} = E_{\alpha}^{\text{P}} - E_{\beta}^{\text{P}}$ ) for  $\alpha$ - vs.  $\beta$ -addition in the gas and solution phases;<sup>b</sup> R, R<sup>1</sup>, and R<sup>2</sup> are defined in Scheme 1

compound	R	R <sup>1</sup>	R <sup>2</sup>	gas phase			solution phase		
				$\Delta E^{\text{TS}}$	$\Delta E^{\text{I}}$	$\Delta E^{\text{P}}$	$\Delta E^{\text{TS}}$	$\Delta E^{\text{I}}$	$\Delta E^{\text{P}}$
1	H	H	H	24.1	36.6	3.5	25.2	38.8	4.7
2 <sup>c</sup>	H	H	OCH <sub>3</sub>	22.5	34.9		21.8	33.7	
3	F	H	H	25.4	43.3	1.0	27.3	42.5	1.4
4 <sup>c</sup>	F	H	OCH <sub>3</sub>	22.8	41.9		24.1	37.0	
5	F	F	H	22.7	31.2	-2.4	25.3	29.6	-3.3
6	CF <sub>3</sub>	H	H	8.7	16.9	-0.7	7.7	18.5	
7	CF <sub>3</sub>	CF <sub>3</sub>	H	-3.5	-4.7	-1.7	-1.6	-1.1	
8	CF <sub>3</sub>	CF <sub>3</sub>	OCH <sub>3</sub>	-6.8	-7.8		-4.1	-7.9	
9	NO <sub>2</sub>	H	H	-1.3	-2.2	-2.0	-0.4	-6.9	-2.1
10	NO <sub>2</sub>	H	OCH <sub>3</sub>	-3.4	-4.7		-5.0	-10.4	
11	CH <sub>2</sub> =CH	H	H	8.9	13.8	1.7	12.0	19.4	2.4
12	FHC=CH	H	H	10.5	18.2	1.3	14.6	23.1	1.3
13	FHC=CH	H	OCH <sub>3</sub>	9.7	20.4			21.3	
14	CF <sub>3</sub> (H)C=CH	H	H	2.3	1.9	1.5	5.6	8.1	1.7
15	OHC(H)C=CH	H	H	-0.4	-4.2	1.0	-1.0	-3.6	1.5
16	NO <sub>2</sub> (H)C=CH	H	H	-5.5	-11.3	0.9	-4.6	-13.1	0.9
17	C <sub>6</sub> H <sub>5</sub>	H	H	5.9	12.6	1.3	10.5	19.3	1.3
18	2-NO <sub>2</sub> -C <sub>6</sub> H <sub>4</sub>	H	H	-1.2	-3.3		3.2	-1.1	
19	3-NO <sub>2</sub> -C <sub>6</sub> H <sub>4</sub>	H	H	2.8	9.6		7.9	15.4	
20	4-NO <sub>2</sub> -C <sub>6</sub> H <sub>4</sub>	H	H	-0.7	1.0	0.9	3.1	0.1	
21	2,4-(NO <sub>2</sub> ) <sub>2</sub> -C <sub>6</sub> H <sub>4</sub>	H	H	-6.0	-12.6		-2.9	-9.9	
22	2-NO <sub>2</sub> -4-CF <sub>3</sub> -C <sub>6</sub> H <sub>3</sub>	H	H	-3.8	-12.2		0.1	-6.3	

<sup>a</sup> Calculations were conducted at the B3LYP//HF/6-31+G(d) level for  $\Delta E^{\text{TS}}$  and  $\Delta E^{\text{I}}$  and at the B3LYP/6-31G(d) level for  $\Delta E^{\text{P}}$ .

<sup>b</sup> Solution calculations were conducted for gas-phase-optimized geometries and used the PCM method with a dielectric constant of 7.58, which is representative of THF. Solution free energies are given. <sup>c</sup> See ref.<sup>[22]</sup>



Scheme 1. Reactants, intermediates, and products for  $\alpha$ - and  $\beta$ -addition reactions for which calculations were performed; compounds are defined in Table 1

intermediates (Scheme 1). For comparison, we also performed calculations on reactants, intermediates, and selected overall products. For simplicity, we focused exclusively on *all-trans* reactants and the most closely related transition states and intermediates. We examined addition only at the  $\alpha$ - and  $\beta$ -carbon atoms, and not at  $\gamma$ -,  $\delta$ -, or carbonyl carbon atoms, even when such addition might be expected. This approach was taken because our goal is to establish trends in the relative likelihood of  $\alpha$ - and  $\beta$ -addition, especially for the cinnamaldehydes.

We chose cyanide anion as the nucleophile for the model reactions. Previous research<sup>[2]</sup> on 1,4- and 1,2-addition to acrolein used this nucleophile, providing a point of com-

parison, and its small size limits the number of conformations to be considered. A general reaction scheme showing reactants, intermediates (A and C), and products (B and D) for both  $\alpha$ - and  $\beta$ -addition is depicted in Scheme 1. Our general expectation is that an EWG will stabilize the negative charge at C <sub>$\beta$</sub>  for the intermediate for  $\alpha$ -addition (C) and also, although to a lesser extent, stabilize the corresponding transition state. An example reaction profile calculated for acrolein (1) is shown in Figure 1. Reactants correspond to the central well, and  $\alpha$ - and  $\beta$ -additions proceed to the left and right, respectively.

The reactants are probably ion-dipole complexes and have been studied theoretically for a few  $\beta$ -addition reactions.<sup>[2]</sup> Determining barrier heights to reactions would require an extensive conformational search for the lowest-energy ion-dipole complex for each model compound, which is a daunting task. This effort is not necessary if we make the assumption that the reactants are the same or very similar for both addition reactions. In that case, the relative favorability of  $\alpha$ - vs.  $\beta$ -addition will depend primarily on the difference between the energies of the transition states for  $\alpha$ - and  $\beta$ -addition (if the reaction is under kinetic control) or between the energies of the corresponding products (in the case of thermodynamic control). When we performed calculations on reactants, we assumed the molecules to be at infinite separation.

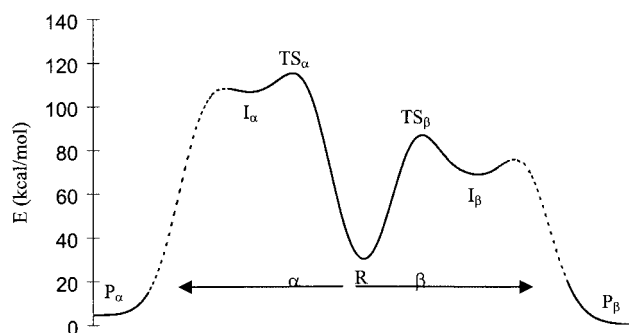
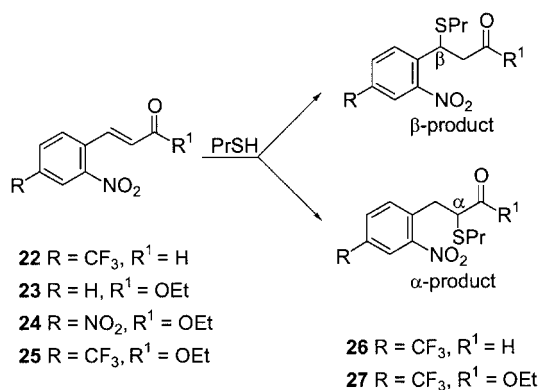


Figure 1. Reaction profile for  $\alpha$ - (to left) and  $\beta$ - (to right) addition of cyanide to **1** in solution (Table 1); reactants correspond to the central well; solid curves are used where energies of stationary points have been calculated [B3LYP//HF/6-31+G(d)]; dashed curves are schematic; energies are relative to  $E_{\beta}^{\text{P}}$ , which is set to zero; R, TS, I, and P represent reactants, transition state, intermediate, and product, respectively; subscripts denote  $\alpha$ - or  $\beta$ -addition; for consistency, energies include a cyanide anion and a THF molecule with the reactants, a protonated THF molecule with the transition states and intermediates, and a THF molecule with the products

**Synthetic Experiments:** A few reactions yielding  $\alpha$ -addition have been reported previously.<sup>[13,14]</sup> In addition, we performed reactions of cinnamic aldehyde **22** and ester **25** with propanethiol. These reactions gave the  $\alpha$ -addition products **26** and **27**, respectively (see Scheme 2 and Exp. Sect.), which confirms the predictions made based on the calculations reported below.



Scheme 2. Michael additions to cinnamic esters and aldehydes for which experimental data are reported here or in the literature; addition of PrSH to compounds **22** and **25** gives  $\alpha$ -adducts **26** and **27**, respectively, as described in the Exp. Sect.; our theoretical calculations confirm that **22** favors  $\alpha$ -addition; the  $\alpha$ -addition of PrSH to **24** and the  $\beta$ -addition to **23** are described in ref.<sup>[14]</sup>

## Computational Methods

Calculations were performed using the GAUSSIAN98 program package.<sup>[17]</sup> Transition states and intermediates were treated with the HF/6-31+G(d) and B3LYP//HF/6-31+G(d) levels of theory. Diffuse functions were omitted for the products because they are neutral species. All stationary points (reactants, intermediates, products, and transition states) were fully optimized. Frequency calcu-

lations confirmed that all transition states had precisely one imaginary frequency.

Solvated calculations used the continuum dielectric method PCM<sup>[16]</sup> with UAHF parameterization and a dielectric constant of 7.58, which is representative of THF.<sup>[18]</sup> Energies given are solution free energies and were evaluated at gas-phase-optimized geometries. Tests using other solvation methods, higher levels of theory, and solution-phase optimization indicated that this method is sufficiently accurate (see Results).

## Results

Table 1 presents differences between energies of transition states ( $\Delta E^{\text{TS}}$ ), of intermediates ( $\Delta E^{\text{I}}$ ), and of selected products ( $\Delta E^{\text{P}}$ ) for  $\alpha$ - vs.  $\beta$ -addition, where  $E_{\alpha}^{\text{TS}}$ ,  $E_{\alpha}^{\text{I}}$ , and  $E_{\alpha}^{\text{P}}$  are the energies of the transition states, intermediates, and products, respectively, for  $\alpha$ -addition, and  $E_{\beta}^{\text{TS}}$ ,  $E_{\beta}^{\text{I}}$ , and  $E_{\beta}^{\text{P}}$  are the corresponding quantities for  $\beta$ -addition.

$$\Delta E^{\text{TS}} = E_{\alpha}^{\text{TS}} - E_{\beta}^{\text{TS}} \quad (1)$$

$$\Delta E^{\text{I}} = E_{\alpha}^{\text{I}} - E_{\beta}^{\text{I}} \quad (2)$$

$$\Delta E^{\text{P}} = E_{\alpha}^{\text{P}} - E_{\beta}^{\text{P}} \quad (3)$$

Under the assumption that reactants are essentially the same for both addition reactions,  $\Delta E^{\text{TS}}$  is equivalent to the difference between the activation energies, where  $E_{\alpha,\alpha}$  and  $E_{\alpha,\beta}$  are the activation energies for  $\alpha$ - and  $\beta$ -addition, respectively, and  $E^{\text{R}}$  is the reactants' energy.

$$E_{\alpha,\alpha} = E_{\alpha}^{\text{TS}} - E^{\text{R}}, E_{\alpha,\beta} = E_{\beta}^{\text{TS}} - E^{\text{R}} \quad (4)$$

$$E_{\alpha,\alpha} - E_{\alpha,\beta} = \Delta E^{\text{TS}} \quad (5)$$

Likewise,  $\Delta E^{\text{P}}$  represents the difference between the overall heats of reaction of  $\alpha$ - and  $\beta$ -addition, and  $\Delta E^{\text{I}}$  represents the difference between the heats of reaction for the initial step only. The sign of  $\Delta E^{\text{TS}}$  indicates which of the reactions is kinetically favored (positive for  $\beta$ -addition, negative for  $\alpha$ -addition), and the sign of  $\Delta E^{\text{P}}$  indicates which of the reactions is thermodynamically favored. As Table 1 demonstrates, trends in  $\Delta E^{\text{I}}$  parallel those in  $\Delta E^{\text{TS}}$ . This finding can be useful because  $\Delta E^{\text{I}}$  is generally easier to compute.

Gas-phase and solution-phase values for  $\Delta E^{\text{TS}}$ ,  $\Delta E^{\text{I}}$ , and  $\Delta E^{\text{P}}$  are given in Table 1. The solution-phase values were calculated at gas-phase-optimized geometries. When needed for clarity, we indicate the phase in parentheses, e.g.,  $E^{\text{TS}}(\text{gas})$  or  $E^{\text{TS}}(\text{soln.})$ . For **1** and **11**,  $\Delta E^{\text{I}}(\text{soln.})$  and  $\Delta E^{\text{TS}}(\text{soln.})$  were calculated at solution-phase- as well as gas-phase-optimized geometries. These values are given in Table 2. Optimizing in solution changes the values of  $\Delta E^{\text{I}}$  and  $\Delta E^{\text{TS}}$  by 1.5 and 2.9 kcal/mol, respectively, or less. These changes are reasonably small relative to the range of values for  $\Delta E^{\text{I}}$  and  $\Delta E^{\text{TS}}$  in Table 1. Solution-phase optimization is much more expensive, particularly for the larger

models, and, furthermore, full equilibrium solvation of transition states is not justified on theoretical grounds.<sup>[19]</sup> For these reasons, all energies in solution are at gas-phase-optimized geometries, except for the examples mentioned above.

Table 2. Solution-phase energy differences<sup>a,b</sup> (kcal/mol) for geometries optimized in the gas phase (conf. 1) or solution phase (conf. 2)

compound	$\Delta E^I$		$\Delta E^{TS}$	
	conf. 1	conf. 2	conf. 1	conf. 2
<b>1</b>	38.83	40.32	25.16	27.68
<b>11<sup>b</sup></b>	19.36	19.89	11.99	14.87

<sup>a</sup> The calculations were conducted at the HF/6-31+G(d) level.

<sup>b</sup> For **11**, solution-phase optimizations for  $\Delta E^I$  and  $\Delta E^{TS}$  did not quite converge, but oscillated within a range of 0.006 kcal/mol.

In Table 3 we compare the values of  $\Delta E^{TS}$  and  $\Delta E^P$  with the zero-point-corrected values ( $\Delta E_{+ZPE}^{TS}$  and  $\Delta E_{+ZPE}^P$ ) for selected compounds **1**, **9**, **11**, **14**, and **16**. The zero-point corrections for  $\alpha$ - and  $\beta$ -addition nearly cancel. For these compounds, the difference between the corrected and uncorrected energies lies in the range 0.2–0.9 kcal/mol for transition states and 0.0–0.3 kcal/mol for products. The average unsigned zero-point correction to  $\Delta E^{TS}$  over all compounds **1–22** is 0.4 kcal/mol. Since these corrections are small relative to the range in values of  $\Delta E^{TS}$  and  $\Delta E^P$  listed in Table 1, we use the uncorrected values for the rest of our analyses.

Table 3. Gas-phase values of  $\Delta E^{TS}$  and  $\Delta E^P$  (kcal/mol) calculated with and without the zero-point energy [B3LYP//HF/6-31+G(d)]

compound	$\Delta E^{TS}$	$\Delta E_{+ZPE}^{TS}$	$\Delta E^P$	$\Delta E_{+ZPE}^P$
<b>1</b>	24.1	23.3	3.5	3.2
<b>9</b>	-1.3	-1.7	-2.0	-1.7
<b>11</b>	8.9	8.3	1.7	1.7
<b>14</b>	2.3	1.8	1.5	1.4
<b>16</b>	-5.5	-5.7	0.9	0.9

To document the accuracy of the calculations, we compared values of  $\Delta E^I$  and  $\Delta E^{TS}$  at the HF/6-31+G(d) and B3LYP//HF/6-31+G(d) levels of theory. We define the difference between values calculated with the two methods as  $\Delta\Delta E^{TS}$  and  $\Delta\Delta E^I$ , i.e.:

$$\Delta\Delta E^{TS} = \Delta E^{TS}(\text{HF}) - \Delta E^{TS}(\text{B3LYP}) \quad (6)$$

where the level of theory is indicated in parentheses;  $\Delta\Delta E^I$  is defined analogously. Values of  $\Delta\Delta E^{TS}$  and  $\Delta\Delta E^I$  are given in Table 4. For comparison, we also calculated differences in the activation energies using the two methods, i.e., for  $\alpha$ -addition:

$$\Delta E_{a,\alpha} = E_{a,\alpha}(\text{HF}) - E_{a,\alpha}(\text{B3LYP}) \quad (7)$$

Table 4. Differences between HF/6-31+G(d) and B3LYP//HF/6-31+G(d) energies (kcal/mol)

compound	$\Delta E_{a,\alpha}$	$\Delta E_{a,\beta}$	$\Delta\Delta E^I$	$\Delta\Delta E^{TS}$
<b>1</b>	12.56	13.08	1.01	0.52
<b>6</b>	12.91	14.75	0.62	1.84
<b>7</b>	11.51	16.78	1.18	5.27
<b>9</b>	8.82	11.96	5.45	3.14
<b>11</b>	13.65	12.26	-3.66	-1.39
<b>14</b>	14.12	13.06	-2.88	-1.07
<b>15</b>	14.62	12.47	-0.09	-2.16
<b>16</b>	13.92	12.73	2.07	-1.19
ave. <sup>a</sup>	12.76	13.39	2.12	2.07

<sup>a</sup> Averages are of unsigned quantities.

The quantity  $\Delta E_{a,\beta}$  for  $\beta$ -addition is defined analogously. The average unsigned values of  $\Delta\Delta E^{TS}$  and  $\Delta\Delta E^I$  are 2.07 and 2.12 kcal/mol, respectively. These values are relatively small when compared to the range of values of  $\Delta E^{TS}$  and  $\Delta E^I$  listed in Table 1. The values of  $\Delta E_{a,\alpha}$  and  $\Delta E_{a,\beta}$  are somewhat larger, in the range 9–17 kcal/mol. We can understand these data in terms of cancellation of error. The similarity of the transition states for  $\alpha$ - and  $\beta$ -addition causes errors due to neglect of electron correlation to largely cancel in  $\Delta E^{TS}$ . For analogous reasons, errors also cancel in  $\Delta E^I$ . On the other hand,  $E_{a,\alpha}$  (or  $E_{a,\beta}$ ) represents the energy difference between species having different kinds and numbers of bonds (reactants vs. transition states), and so we would not expect errors to cancel to as great an extent. Cancellation of error is well known and, in fact, sought after in quantum chemistry. For example, heats of reaction calculated at a given level of theory are most accurate for isodesmic reactions, whose reactants and products have the same kinds and numbers of bonds (as do the  $\alpha$ - and  $\beta$ -addition transition states discussed here).<sup>[19]</sup>

We also calculated values of  $\Delta E^I$  and  $\Delta E^{TS}$  for **6** and **11** at the B3LYP/6-31+G(d) level. On average, the values increased by 1.90 and 1.85 kcal/mol, respectively, relative to the values listed in Table 1. These are relatively small changes when compared to the range of values listed in Table 1. For these reasons, the levels of theory chosen here are sufficiently accurate to evaluate the trends in reactivity that are of interest to us.

We also evaluated the quality of the calculations by examining transition state geometries. The most important distances and angles are defined in Figure 2. In Figure 2 and in the following discussion,  $C_C$  and  $C_N$  represent the carbonyl carbon and the carbon of the attacking nucleophile, respectively. Values of the distances and angles are given in Table 5 for the subset of compounds used to compare the levels of theory (vide supra). The stereoelectronic requirements for Michael addition include a  $C_N C_\beta C_\alpha$  attack angle,  $\theta$ , of 100–110° (the ‘‘Burgi–Dunitz attack angle’’<sup>[21]</sup>) and a  $C_N C_\beta C_\alpha C_C$  torsional angle,  $\phi$ , of ca. 90°. In our calculations on  $\beta$ -addition, the value of  $\theta$  for the transition state varies between 107 and 120°. This range is slightly larger than the ideal Burgi–Dunitz attack angle, but values slightly larger than 110° have been obtained before in theor-



etical calculations.<sup>[2]</sup> The values of  $\phi$  for  $\beta$ -addition are quite close to  $90^\circ$  (only the magnitude matters). Similar values are obtained for transition states for  $\alpha$ -addition when  $\theta$  and  $\phi$  are defined analogously as per Figure 2. We conclude that our transition state geometries are consistent with the stereoelectronic requirements for Michael addition.

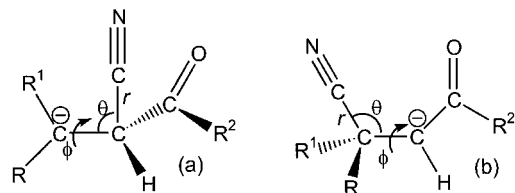


Figure 2. Definitions of geometrical data for (a)  $\alpha$ -addition and (b)  $\beta$ -addition; in (a),  $\phi$  is the  $C_N-C_\alpha-C_\beta-R$  torsion angle; in (b),  $\phi$  is the  $C_N-C_\beta-C_\alpha-C_C$  torsion angle

Table 5. Geometric data,<sup>a</sup> defined in Figure 2, for transition states for  $\alpha$ - and  $\beta$ -addition

compound	$\alpha$ -addition			$\beta$ -addition		
	$r$	$\theta$	$\phi$	$r$	$\theta$	$\phi$
1	1.833	118.4	-76.5	2.053	117.6	-91.3
6	1.943	117.5	-82.8	2.097	115.4	-90.5
7	2.068	116.8	-86.0	2.091	114.2	-89.8
9	2.113	114.6	-91.7	2.068	118.2	-93.4
11	1.893	116.6	-88.0	2.035	114.3	-90.3
14	2.034	114.9	-92.0	2.032	115.2	-91.1
15	2.064	114.6	-95.5	2.026	115.3	-92.1
16	2.106	114.3	-95.1	2.025	116.0	-91.8

<sup>a</sup> Distances are in Angstroms, and angles are in degrees.

We also evaluated the relationship between the length of the partially formed carbon–carbon bond in the transition state,  $R_{CC}$ , and the heat of reaction for creation of the intermediate, where  $\Delta_R H^1$  is the heat of reaction for the first step of the addition reaction (either  $\alpha$  or  $\beta$ ).

$$\Delta_R H^1 = E^I - E^R \quad (8)$$

Our choice of reactants (at infinite separation, rather than an ion–dipole complex) shifts all heats of reaction by some approximately constant amount, but still reveals trends with respect to relative exothermicity. In Figure 3,  $R_{CC}$  is plotted vs.  $\Delta_R H^1$  for  $\alpha$ - and  $\beta$ -addition, in both the gas and solution phases. We see that  $R_{CC}$  is inversely related to the exothermicity, which is consistent with the Hammond postulate.<sup>[21]</sup> The greater scatter in the solution-phase data may be due to the geometries having been optimized in the gas phase. The  $\alpha$ -additions exhibit greater variation than the  $\beta$ -additions in values of both  $\Delta_R H^1$  and  $R_{CC}$ , which indicates that the  $\alpha$ -additions are more sensitive to the nature of the EWG attached to  $C_\beta$ .

## Discussion

Table 1 shows a clear trend for values of  $\Delta E^{TS}$ ,  $\Delta E^I$ , and  $\Delta E^P$  decreasing as the strength of the EWG increases ( $\text{NO}_2$

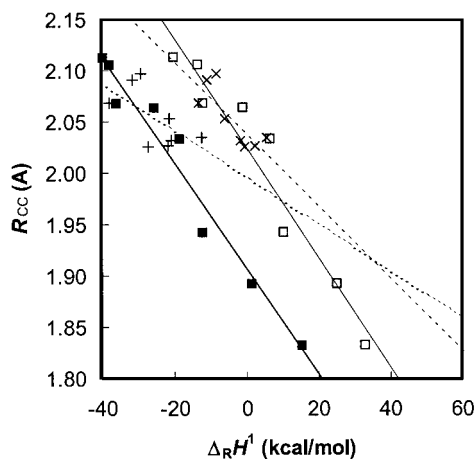


Figure 3. Length ( $R_{CC}$ ) of partially formed C–C bond vs. heat of reaction for the first step of reaction, which here is approximated as  $\Delta_R H^1 = E^I - E^R$ , where  $E^R$  is the energy of the isolated reactants; the solid squares and heavy solid line represent gas-phase  $\alpha$ -addition; the open squares and light solid line represent solution-phase  $\alpha$ -addition; the pluses and heavy dashed line represent gas-phase  $\beta$ -addition; and the crosses and light dashed line represent solution-phase  $\beta$ -addition

$> \text{CHO} > \text{CF}_3 > \text{F}$ ). The trend is more pronounced for  $\Delta E^{TS}$  and  $\Delta E^I$  than for  $\Delta E^P$ . We believe that this finding occurs because the transition states and intermediates carry a charge, and  $\Delta E^{TS}$  and  $\Delta E^I$  reflect the preference for localization of the charge on the  $C_\alpha$  or the  $C_\beta$  side. For the propenals **1**, **3**, **5–7**, and **9**, both  $\Delta E^{TS}$  and  $\Delta E^P$  change sign as the strength of the electron-withdrawing group increases, which suggests a change in the regioselectivity from  $\beta$ - to  $\alpha$ -addition. The magnitudes of  $\Delta E^P$ , however, are small relative to the uncertainties in the calculated values, and cannot be considered a conclusive measure of the relative thermodynamic favorability of  $\alpha$ - vs.  $\beta$ -addition. For the pentadienals and cinnamaldehydes, all of the calculated  $\Delta E^P$  values are positive. Furthermore, the effect of the EWGs on  $\Delta E^P$  decreases with respect to the number of bonds in the conjugated system that separate the EWG from the  $\beta$ -carbon atom. The nitro group decreases  $\Delta E^P(\text{gas})$  for **9** relative to **1** by 5.5 kcal/mol, for **16** relative to **11** by 0.8 kcal/mol, and for **20** relative to **17** by only 0.4 kcal/mol. Thus, the value of  $\Delta E^P$  does not appear to explain why  $\alpha$ -addition is observed experimentally for some polysubstituted cinnamates and cinnamaldehydes. By contrast,  $\Delta E^{TS}$  does become negative for pentadienals and cinnamaldehydes when the EWGs are sufficiently strong. We conclude that  $\Delta E^{TS}$ , rather than  $\Delta E^P$ , is predictive of the regioselectivity, which thus appears to be under kinetic control.

On the basis of the value of  $\Delta E^{TS}$ , the presence of two  $\text{CF}_3$  groups or one  $\text{NO}_2$  group is sufficient to favor  $\alpha$ -addition for the propenals and methyl propenoate **3–10**. A single  $\text{NO}_2$  group is also sufficient to favor  $\alpha$ -addition for the pentadienals and methyl pentadienoate (**11–16**). For the cinnamaldehydes **17–22**, two  $\text{NO}_2$  groups or one  $\text{NO}_2$  group plus one  $\text{CF}_3$  group is needed to favor  $\alpha$ -addition. The influence of EWGs diminishes as the number of bonds separating the EWGs from  $C_\beta$  increases, but  $\alpha$ -addition is

possible even for the cinnamaldehydes if the phenyl ring is multiply substituted.

**Solvation:** For acrolein (**1**), solvation increases the values of  $\Delta E^I$  and  $\Delta E^{TS}$  relative to their values in the gas phase. The  $\pi$  electrons are more delocalized and, hence, more polarizable in the intermediate **A** for  $\beta$ -addition than in the intermediate **C** for  $\alpha$ -addition. This effect allows greater solvent stabilization of the intermediate for  $\beta$ -addition. (The change in the dipole moment upon going from the gas phase to the solution phase is 1.0 Debye for the  $\beta$ -addition intermediate vs. 0.3 Debye for the  $\alpha$ -addition intermediate at the B3LYP//HF/6-31+G(d) level.) The influence of solvation on the value of  $\Delta E^{TS}$  is smaller than it is on  $\Delta E^I$ , presumably because the transition states more closely resemble the reactants. (The reactants for the two additions are the same when neglecting small differences in ion-dipole complexes.) Similar effects are observed for the compounds having unsubstituted vinyl (**11**) and phenyl substituents (**17**). When EWGs are present, competing influences must be considered, and it becomes more difficult to rationalize the effect of solvation on  $\Delta E^I$  and  $\Delta E^{TS}$ .

**Methyl Esters:** The methyl esters ( $R^2 = OCH_3$ ) generally display the same trends as the aldehydes. Therefore, we focused our computational efforts on aldehydes for reasons of cost. We note, however, that the esters have smaller values of  $\Delta E^{TS}$  and  $\Delta E^I$  than the corresponding aldehydes with one exception [ $\Delta E^I(\text{gas})$  for **13**]. We attribute this phenomenon to destabilization of the transition state and intermediate for  $\beta$ -addition by  $\pi$ -donation from the methyl ester unit. Thus, esters may be slightly more effective promoters of  $\alpha$ -addition than are aldehydes.

**EWG F:** Attaching a single F atom to  $C_\beta$  (**3** vs. **1** and **4** vs. **2**) increases the values of  $\Delta E^I$  and  $\Delta E^{TS}$ . We attribute this effect to destabilization of the intermediate and transition state for  $\alpha$ -addition by fluorine's  $\pi$ -donating character (polarity is also a factor in solution). Likewise,  $\Delta E^I$  and  $\Delta E^{TS}$  for **12** are increased relative to **11**. Attaching a second fluorine atom to  $C_\beta$  (**5**), however, decreases the values of  $\Delta E^{TS}$  and  $\Delta E^I$  relative to these values for **3**. These countervailing effects are probably results of fluorine's dual character a  $\pi$ -donator and a  $\sigma$ -withdrawer. In any case, we find that an F atom is less effective than the other EWGs in promoting  $\alpha$ -addition.

**EWG  $CF_3$ , CHO, and  $NO_2$ :** A single trifluoromethyl group at  $C_\beta$  (**6**) decreases the values of  $\Delta E^{TS}$  and  $\Delta E^I$  in the gas phase by 15.4 and 19.7 kcal/mol, respectively, relative to these values for **1**. These changes are substantial, but they are insufficient to make  $\alpha$ -addition favorable. A second trifluoromethyl group at  $C_\beta$  (**7**) further decreases the values of  $\Delta E^{TS}$  and  $\Delta E^I$  in the gas phase by 12.2 and 21.6 kcal/mol, respectively. Thus, the effects of the two trifluoromethyl groups are nearly additive. The same trends are also observed in solution. In particular, the value of  $\Delta E^{TS}$  for **7** is negative. Thus,  $\alpha$ -addition is predicted to occur, which is consistent with the experimental result<sup>[13]</sup> found using the corresponding methyl ester, **8**.

The influence of a single nitro group (**9**) on  $\Delta E^{TS}$  is about the same as that of two trifluoromethyl groups. Although

the aldehyde group,  $R = CHO$ , is not included among models **1–10**,  $\Delta E^I$  and  $\Delta E^{TS}$  must be zero by symmetry considerations. This finding is consistent with the EWGs' strengths ( $NO_2 > CHO > CF_3$ ) as reflected in the values of  $\Delta E^I$  and  $\Delta E^{TS}$  for **6** and **9**. Energies for  $R = CHO$  are given in the Supporting Information (see also the footnote on the first page of this article).

The regioselectivity of nucleophilic attack reflects a competition between the electron-withdrawing strengths of groups attached to  $C_\alpha$  and  $C_\beta$ . For example, in **9**, the  $NO_2$  group attached to  $C_\beta$  has a greater electron-withdrawing strength than the CHO group attached to  $C_\alpha$ . Consistent with this finding,  $\alpha$ -addition is predicted by the negative sign of  $\Delta E^{TS}$ . Note that nitro olefins and trifluoromethyl-substituted olefins are known to undergo Michael addition at the carbon atom  $\beta$  with respect to the nitro or trifluoromethyl group. Reactions of nitro olefins have been studied theoretically.<sup>[6]</sup>

The trends just described for **1–10** are also exhibited by the pentadienals and pentadienoate **11–16**. A trifluoromethyl (**14**) or nitro (**16**) group attached to the  $\delta$ -carbon atom reduces the values of  $\Delta E^I$  and  $\Delta E^{TS}$  relative to those of **11**, with the nitro group to a greater extent, just as the values of  $\Delta E^I$  and  $\Delta E^{TS}$  for **6** and **9** are reduced relative to **1**. The aldehyde group (**15**) is again intermediate between the trifluoromethyl and nitro groups in promoting  $\alpha$ -addition. The influence of the EWGs is smaller when they are separated from  $C_\beta$  by the extra double bond. To recognize this, it is important to note that the "baseline" has shifted: the values of  $\Delta E^I$  and  $\Delta E^{TS}$  for the unsubstituted vinylic model, **11**, are reduced relative to those of **1** as a result of resonance stabilization of the intermediate and transition state for  $\alpha$ -addition.

Next we turn to the cinnamaldehydes, **17–22**. From the work described above, we expected that single substitution of the phenyl ring by an F atom or  $CF_3$  group would be insufficient to favor  $\alpha$ -addition. Consequently we focused on phenyl rings singly substituted with  $NO_2$  or multiply substituted with  $NO_2$  and  $CF_3$ . Of the mononitrophenyl compounds, the 3-nitrophenyl compound, **19**, has the smallest influence on the values of  $\Delta E^I$  and  $\Delta E^{TS}$ , and the 2- and 4-nitrophenyl compounds, **18** and **20**, have similar influences, as one would expect. The sign of  $\Delta E^{TS}(\text{soln.})$  is in agreement with the experimental finding<sup>[14]</sup> that mononitro-substituted cinnamate **23** undergoes  $\beta$ -addition (Scheme 2). The magnitude of  $\Delta E^{TS}(\text{soln.})$ , however, is small for **18** and **20**, which suggests that adding more EWGs to the phenyl ring will favor  $\alpha$ -addition. This effect is clearly the case for the 2,4-dinitro-substituted compound, **21**, because  $\Delta E^{TS}(\text{soln.})$  is negative. This result is in agreement with the experimental finding<sup>[14]</sup> that the ethyl ester, **24**, undergoes  $\alpha$ -addition with propanethiol. On the basis of these results, we predicted that even one trifluoromethyl group in addition to a 2-nitro or 4-nitro group (e.g., **22**) would be sufficient to favor  $\alpha$ -addition. The calculated value of  $\Delta E^{TS}(\text{gas})$  for **22** ( $-3.8$  kcal/mol) favors  $\alpha$ -addition, while the value of  $\Delta E^{TS}(\text{soln.})$  (0.1 kcal/mol) is inconclusive.

**Experimental Evidence for  $\alpha$ -Additions:** We performed several nucleophilic addition reactions with  $\alpha,\beta$ -unsaturated carbonyl compounds having a multiply substituted phenyl ring attached to  $C_\beta$  (Scheme 2). Reaction of **25** with propantethiol gave a single  $\alpha$ -addition product, **27**, whose structure was confirmed by 2D NMR spectroscopy experiments. The high-resolution mass spectrum of **27** showed, in addition to the molecular ion, a peak for an ion at  $m/z = 161.0632$  whose elemental composition,  $C_7H_{13}O_2S$  ( $C_3H_7SCHCO_2C_2H_5$ )<sup>+</sup>, further supports the occurrence of  $\alpha$ -addition of the thiol to the  $\alpha,\beta$ -unsaturated ester **25**. Analogously, addition of propantethiol to **22** gave a single  $\alpha$ -addition product, **26**.

**Factors Controlling the Regioselectivity:** To understand the factors controlling the regioselectivity, we related the values of  $\Delta E^{TS}$  to properties of the reacting species. The analysis is based on fitting the values of  $\Delta E^{TS}$  by a simple expression in terms of partial atomic charges and contributions to frontier orbitals:

$$\Delta E_{fit}^{TS} = A(Q(C_\alpha) - Q(C_\beta)) + B \frac{(\sum_a c_a^2 - \sum_b c_b^2)}{E_{HOMO(nuc.)} - E_{LUMO(elec.)}} + C \quad (9)$$

where  $Q(X)$  is the partial atomic charge on atom X in the isolated molecule;  $a$  and  $b$  label atomic orbitals centered on atoms  $C_\alpha$  and  $C_\beta$ , respectively;  $c_a$  ( $c_b$ ) is the coefficient of atomic orbital  $a$  ( $b$ ) in the electrophile's LUMO;  $E_{HOMO(nuc.)}$  and  $E_{LUMO(elec.)}$  are the energies of the nucleophile's HOMO and the electrophile's LUMO, respectively; and  $A$ ,  $B$ , and  $C$  are empirical fitting parameters. Equation (9) is based on a perturbation theory expression<sup>[12]</sup> for the energy of the transition state. We postulate that Equation (9), although a considerable simplification, will capture the dominant effects.

To implement Equation (9), values of  $E_{HOMO(nuc.)}$  and  $E_{LUMO(elec.)}$  and the partial atomic charges were determined from HF/6-31+G(d) calculations at the gas-phase-optimized geometries. (Interpretation of Kohn-Shan orbitals from B3LYP calculations is ambiguous.) The charges were calculated using the CHelpG method.<sup>[23]</sup> The atomic orbital coefficients  $c_a$  and  $c_b$  were determined by HF/6-31G single-point calculations [assigning electron probability density to atoms in molecules on the basis of loose, e.g., diffuse (+) or d, functions can be deceptive]. A typical set of LUMO coefficients (for **11**) for basis functions centered on  $C_\alpha$  or  $C_\beta$  is given in Table 6.

Since most of the model compounds are planar and attack occurs from above or below the plane of the molecule (defined as the  $xy$  plane), the most important contributions to the LUMO are from  $p_z$  basis functions. For the 6-31G basis set, each heavy atom has two sets of p-type basis functions, the tighter labeled 2p and the looser labeled 3p. Note that, for **11**, the magnitudes of the  $2p_z$  and  $3p_z$  coefficients are larger for  $C_\beta$  than they are for  $C_\alpha$ , which is consistent with  $\beta$ -addition being favored ( $\Delta E^{TS} > 0$ ). For simplicity, we have included only the 3p coefficients in the sum in

Table 6. Coefficients of the basis functions centered on  $C_\alpha$  and  $C_\beta$  to the LUMO for **11** (HF/6-31G)

basis function	$C_\alpha$	$C_\beta$
1s	0.00000	0.00000
2s	-0.00001	0.00001
2p <sub>x</sub>	0.00002	-0.00002
2p <sub>y</sub>	-0.00003	0.00003
2p <sub>z</sub>	0.21271	-0.27960
3s	-0.00003	-0.00001
3p <sub>x</sub>	-0.00001	-0.00006
3p <sub>y</sub>	-0.00007	0.00001
3p <sub>z</sub>	0.32046	-0.38634

Equation (9) because they are larger and, 3p basis functions being looser, they contribute more to orbital overlap. In most cases, the values of  $3p_x$  and  $3p_y$  were very small. The *ortho* substituents, however, for **18**, **21**, and **22** cause distortions from planarity and, consequently, the  $3p_x$  and  $3p_y$  coefficients were not negligible.

We performed gas- and solution-phase fits to the set of all compounds (Figures 4 and 5, respectively), and also gas-phase fits individually to the propenals (Figure 6), the pen-

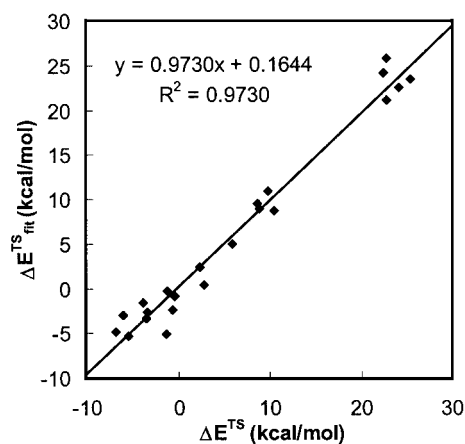


Figure 4. Fitted vs. ab initio values of  $\Delta E^{TS}$  for Fit 5 (to compounds **1**–**22** in the gas phase); the equation of the best-fit line to these data and the correlation coefficient,  $R^2$ , are given

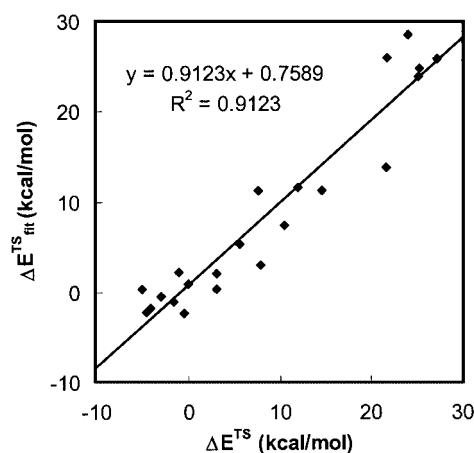


Figure 5. As defined for Figure 4, but for Fit 6 [to  $\Delta E^{TS}(\text{soln.})$ ]

tadienals, the methyl esters, and the cinnamaldehydes (Figure 7). Figures 4–7 depict  $\Delta E_{\text{fit}}^{\text{TS}}$ , the value of  $\Delta E^{\text{TS}}$  obtained with Equation (9) using the fitted parameters, vs. the value of  $\Delta E^{\text{TS}}$  from Table 1. In Table 7, the parameters *A*, *B*, and *C* are given and the fits are numbered for reference. The value of *B* is consistent across the fits and is an order-of-magnitude larger than *A* except for Fit 4 (ignoring the sign). Thus, the frontier orbital term dominates for **1–16**, but the charge term is important for the cinnamaldehydes.

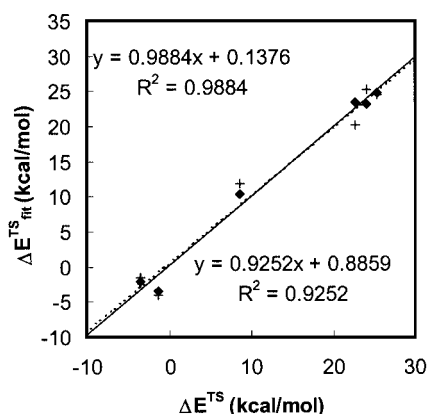


Figure 6. Fitted vs. ab initio values of  $\Delta E^{\text{TS}}$  for gas-phase fits to the propenals **1**, **3**, **5**, **6**, **7** and **9**; the solid diamonds and solid line are for Fit 1, which includes all terms in Equation (9); the equation of the best-fit line to these data and the correlation coefficient,  $R^2$ , are given in the upper left-hand corner; the pluses and dashed line are for a fit with the charge term excluded; the equation of the best-fit line to these data and the  $R^2$  value are given in the lower right-hand corner

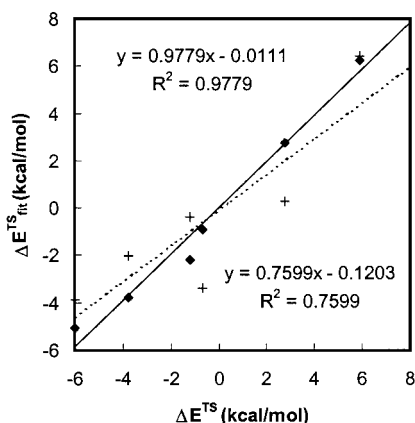


Figure 7. Fitted vs. ab initio values of  $\Delta E^{\text{TS}}$  for the cinnamaldehydes **17–22** in the gas phase; the meaning of types of lines and symbols is as defined in Figure 6

Fit 1, to the propenals (solid line and solid diamonds in Figure 6), is excellent (the correlation coefficient,  $R^2$ , is 0.9884). A fit with the charge term excluded (dashed line and pluses) is only slightly poorer ( $R^2 = 0.9252$ ). We conclude that the frontier term is dominant, as Table 7 suggests. Fits to the pentadienals (graphs not shown) are of similarly good quality with or without the charge term [ $R^2$  is 0.9903 (Fit 2) and 0.9899, respectively], as are fits to all

Table 7. Parameters<sup>a</sup> from fits to Equation (9)

Fit	Compounds <sup>b</sup>	<i>A</i>	<i>B</i>	<i>C</i>
1	<b>1,3,5,6,7,9</b> <sup>c,d</sup>	-3.47	33.75	3.10
2	<b>11,12,14-16</b> <sup>d,e</sup>	2.15	33.75	3.10
3	<b>2,4,8,10,13</b> <sup>d,f</sup>	-0.58	35.00	0.54
4	<b>17-22</b> <sup>d,g</sup>	-39.04	33.86	5.12
5	<b>1-22</b> <sup>d</sup>	-2.35	35.02	1.63
6	<b>1-22</b> <sup>h</sup>	-3.81	33.26	4.20

<sup>a</sup> The units of *A*, *B*, and *C* are kcal/mol when charges and orbital energies in Equation (9) have their numerical values in atomic units. <sup>b</sup> Compounds included in the fit. <sup>c</sup> Propenals. <sup>d</sup> Gas phase. <sup>e</sup> Pentadienals. <sup>f</sup> Methyl esters. <sup>g</sup> Cinnamaldehydes. <sup>h</sup> Solution phase.

of the methyl esters [ $R^2$  is 0.9983 (Fit 3) and 0.9982, respectively]. By contrast, a fit to the cinnamaldehydes is much poorer without the charge term [ $R^2$  is 0.9779 with (Fit 4) and 0.7599 without]. This finding is consistent with the results listed in Table 7 in indicating that the charge term is important for determining the regioselectivity for the cinnamaldehydes.

The gas-phase fit to all compounds in Figure 4 [Fit 5, which uses all terms in Equation (9)] has a little more scatter than Fits 1–4, but it is still quite good ( $R^2 = 0.9730$ ). The corresponding solution-phase fit (Figure 5) is surprisingly poor ( $R^2 = 0.7551$ ). This feature is traceable to the LUMO  $3p_z$  coefficients for **7** and **8**, which are larger for  $C_\beta$  than they are for  $C_\alpha$  even though  $\Delta E^{\text{TS}}(\text{soln.})$  is negative. This anomaly occurs only when trifluoromethyl groups are attached directly to  $C_\beta$ . A fit of  $\Delta E^{\text{TS}}(\text{soln.})$  using gas-phase charge and frontier orbital data (Fit 6) yields a much better fit ( $R^2 = 0.9123$ ). If **7** and **8** are excluded, fits of  $\Delta E^{\text{TS}}(\text{soln.})$  using gas-phase and solution-phase data are of nearly identical quality ( $R^2$  is 0.9040 and 0.8828, respectively).

Figure 8 shows the contributions of the individual charge and frontier terms to  $\Delta E_{\text{fit}}^{\text{TS}}$  for Fit 5. Beta-addition to acrolein, **1**, is understood to be under frontier control,<sup>[2]</sup> which is consistent with the dominance of the frontier term as depicted in Figure 8. The frontier term is dominant in all

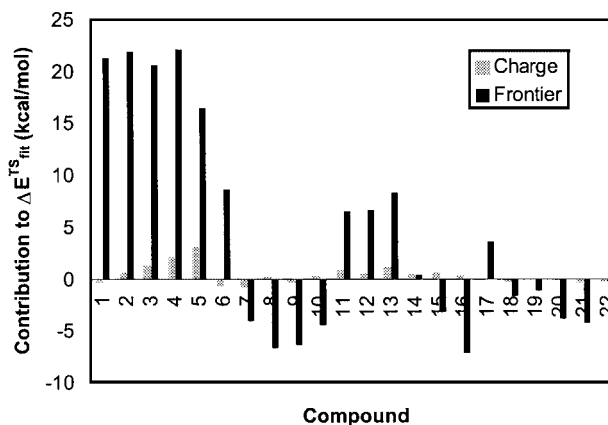


Figure 8. Charge and frontier contributions to  $\Delta E_{\text{fit}}^{\text{TS}}$  from Fit 5 (Figure 4 and Table 7)



cases except **14**, although some EWGs, notably the F atom, increase the charge contribution. (The cinnamaldehydes appear to have small charge contributions here because Figure 8 reflects Fit 5. A similar figure based on Fit 4, however, which is a fit to the cinnamaldehydes alone, would show much larger charge contributions.) It is particularly intriguing when the charge and frontier terms have the opposite sign (e.g., **15**), as this phenomenon suggests that the regioselectivity may be particularly sensitive to the solvent polarity or the choice of a hard vs. a soft nucleophile.

The fits suggest that these reactions are under frontier control, but that charge is significant in some cases, particularly for the cinnamaldehydes. This finding could help to guide the choice of solvent and nucleophile. The fits provide parameters that can be used to predict the regioselectivity from easily calculated properties of reactants. In particular, Fits 5 and 6 provide parameters that are applicable to a wide variety of  $\alpha,\beta$ -unsaturated carbonyl compounds. For cinnamaldehydes, however, it is preferable to use the parameters from Fit 4.

## Conclusion

The theoretical results presented here are consistent with those from experiments and suggest that the site of nucleophilic attack on an  $\alpha,\beta$ -unsaturated carbonyl compound can be finely controlled by the selection of electron-withdrawing groups. In particular, these results indicate that the presence of one nitro group or two trifluoromethyl groups at carbon atom  $\beta$  reverses the polarity of the carbon-carbon double bond in acrolein acceptors and redirects the regioselectivity of nucleophilic addition from the classical  $\beta$ -addition to an abnormal  $\alpha$ -addition. Two nitro groups, or one nitro group plus one trifluoromethyl group, on a phenyl ring attached to carbon atom  $\beta$  have an analogous effect on nucleophilic addition to cinnamaldehydes.

We have shown that the influence of particular electron-withdrawing groups on the regioselectivity of attack follows established trends in electron-withdrawing strength ( $\text{NO}_2 > \text{CHO} > \text{CF}_3 > \text{F}$ ). Separation from  $\text{C}_\beta$  by an intervening conjugated system reduces the influence on relative barrier heights, but  $\alpha$ -addition can be favored even for a phenyl ring if it is multiply substituted. From a fit based on properties of the reactants, we have related the regioselectivity quantitatively to charge and frontier orbital influences. This study provides a simple way to predict likely candidates for  $\alpha$ -addition and suggests that the regioselectivity may be sensitive to the hardness or softness of the nucleophile, particularly for the cinnamaldehydes.

## Experimental Section

$^1\text{H}$  (400 MHz),  $^{13}\text{C}$  (100 MHz), and  $^{19}\text{F}$  [376.5 MHz ( $\text{CFCl}_3$ )] NMR spectra were determined from solutions of compounds in  $\text{CHCl}_3$ . Mass spectra (MS and HR-MS) were obtained using the electron impact mode (EI, 20 eV). Elemental analyses were determined at the Microanalytical Laboratory at Adam Mickiewicz Uni-

versity, Poznan, Poland. Merck Kieselgel 60-F<sub>254</sub> sheets were used for TLC and products were detected with 254-nm light. Merck Kieselgel 60 (230–400 mesh) was used for column chromatography. Cinnamic ester **25** and aldehyde **22** were prepared by condensation of 2-nitro-4-(trifluoromethyl)benzaldehyde with ethoxycarbonylmethylene- and formylmethylene-stabilized Wittig reagents as described below.

**(E)-3-[2-Nitro-4-(trifluoromethyl)phenyl]propenal (22):** (Formylmethylene)triphenylphosphorane (0.21 g, 0.68 mmol) was added in one portion to a stirred solution of 2-nitro-4-(trifluoromethyl)benzaldehyde<sup>[14]</sup> (0.15 g, 0.68 mmol) in anhydrous  $\text{CH}_3\text{CN}$  (6 mL). The resulting solution was stirred overnight at ambient temperature and then the solvent was evaporated. The residue was column chromatographed ( $\text{MeOH}/\text{CH}_2\text{Cl}_2$ , 1:49) to give **22** (0.16 g, 94%) as a solidified oil. IR ( $\text{CHCl}_3$ ):  $\tilde{\nu} = 1690, 1622 \text{ w cm}^{-1}$ .  $^1\text{H}$  NMR:  $\delta = 6.68$  (dd,  $J = 16.0, 7.5 \text{ Hz}$ , 1 H), 7.84 (d,  $J = 8.1 \text{ Hz}$ , 1 H), 7.99 (d,  $J = 8.1 \text{ Hz}$ , 1 H), 8.07 (d,  $J = 16.0 \text{ Hz}$ , 1, CH), 8.42 (s, 1 H), 9.84 (d,  $J = 7.5 \text{ Hz}$ , 1 H) ppm.  $^{13}\text{C}$  NMR:  $\delta = 122.9$  (q,  $^1J = 273.6 \text{ Hz}$ ), 123.1 (q,  $^3J = 3.6 \text{ Hz}$ ), 130.6, 130.8 (q,  $^3J = 3.6 \text{ Hz}$ ), 133.5 (q,  $^2J = 34.5 \text{ Hz}$ ), 133.9, 134.5, 145.9, 193.0 ppm.  $^{19}\text{F}$  NMR:  $\delta = -63.6$  (s) ppm. MS (EI):  $m/z = 245$  (5) [ $\text{M}^+$ ], 216 (75) [ $\text{M}^+ - 29$ ].  $\text{C}_{10}\text{H}_6\text{F}_3\text{NO}_3$  (245.16): calcd. C 48.99, H 2.47, N 5.71; found C 49.17, H 2.57, N 5.65.

**Ethyl (E)-3-[2-Nitro-4-(trifluoromethyl)phenyl]propenoate (25):** Treatment of 2-nitro-4-(trifluoromethyl)benzaldehyde<sup>[14]</sup> (0.15 g, 0.68 mmol) in anhydrous  $\text{CH}_3\text{CN}$  (6 mL) with (ethoxycarbonylmethylene)triphenylphosphorane (0.26 g, 0.75 mmol), using the procedure described for **22**, gave **25** (0.19 g, 96%) as an oil that solidified. IR ( $\text{CHCl}_3$ ):  $\tilde{\nu} = 1716, 1627 \text{ w cm}^{-1}$ .  $^1\text{H}$  NMR:  $\delta = 1.37$  (t,  $J = 7.1 \text{ Hz}$ , 3 H), 4.33 (q,  $J = 7.1 \text{ Hz}$ , 2 H), 6.45 (d,  $J = 15.8 \text{ Hz}$ , 1 H), 7.80 (d,  $J = 8.1 \text{ Hz}$ , 1 H), 7.93 (d,  $J = 8.1 \text{ Hz}$ , 1 H), 8.13 (d,  $J = 15.8 \text{ Hz}$ , 1 H), 8.35 (s, 1 H) ppm.  $^{13}\text{C}$  NMR:  $\delta = 14.6, 61.7, 122.8$  (q,  $^3J = 3.6 \text{ Hz}$ ), 123.1 (q,  $^1J = 273.5 \text{ Hz}$ ), 125.8, 130.5 (q,  $^3J = 3.6 \text{ Hz}$ ), 130.6, 132.8 (q,  $^2J = 34.5 \text{ Hz}$ ), 134.6, 148.4, 165.7 ppm.  $^{19}\text{F}$  NMR:  $\delta = -63.6$  (s) ppm. MS (EI):  $m/z = 289$  (10) [ $\text{M}^+$ ], 244 (50) [ $\text{M}^+ - 45$ ].  $\text{C}_{12}\text{H}_{10}\text{F}_3\text{NO}_4$  (289.21): calcd. C 49.84, H 3.49, N 4.84; found C 49.67, H 3.57, N 4.75.

**3-[2-Nitro-4-(trifluoromethyl)phenyl]-2-(propylthio)propanal (26):** Propanethiol (0.12 mL, 0.1 g, 1.33 mmol) and triethylamine (0.02 mL, 0.015 g, 0.16 mmol) were added sequentially to a stirred solution of **22** (83 mg, 0.34 mmol) in anhydrous THF (4 mL) at ambient temperature. The mixture was left to stand for 24 h and then evaporated to dryness under vacuum. The residue was chromatographed (hexane  $\rightarrow$  2% EtOAc/hexane) to give **26** (70 mg, 64%) as a yellow oil. IR ( $\text{CHCl}_3$ ):  $\tilde{\nu} = 1692 \text{ cm}^{-1}$ .  $^1\text{H}$  NMR:  $\delta = 0.97$  (t,  $J = 7.4 \text{ Hz}$ , 3 H), 1.54–1.58 (m, 2 H), 2.42 (m, 2 H), 3.24 (dd,  $J = 12.6, 5.9 \text{ Hz}$ , 1 H), 3.60 (dd,  $J = 12.6, 7.2 \text{ Hz}$ , 1 H), 3.64 (ddd,  $J = 9.5, 7.2, 2.3 \text{ Hz}$ , 1 H), 7.63 (d,  $J = 8.0 \text{ Hz}$ , 1 H), 7.84 (dd,  $J = 8.0, 1.2 \text{ Hz}$ , 1 H), 8.28 (s, 1 H), 9.44 (d,  $J = 2.2 \text{ Hz}$ , 1 H) ppm.  $^{13}\text{C}$  NMR:  $\delta = 13.7, 23.1, 31.9, 32.5, 53.7, 122.8$  (q,  $^3J = 3.6 \text{ Hz}$ ), 123.2 (q,  $^1J = 273.5 \text{ Hz}$ ), 129.8 (q,  $^3J = 3.6 \text{ Hz}$ ), 131.5 (q,  $^2J = 34.5 \text{ Hz}$ ), 135.0, 137.5, 149.6, 192.2 ppm.  $^{19}\text{F}$  NMR:  $\delta = -63.4$  (s) ppm. HRMS (EI):  $m/z = 321.0635$  (10,  $\text{M}^+$  [ $\text{C}_{13}\text{H}_{14}\text{F}_3\text{NO}_3\text{S}$ ] = 321.0646), 117.0363 {30, [ $\text{C}_5\text{H}_9\text{OS}$ ] = 117.0374,  $\text{CH}(\text{SPr})\text{CHO}$ }.  $\text{C}_{13}\text{H}_{14}\text{F}_3\text{NO}_3\text{S}$  (321.32): calcd. C 48.59, H 4.39, N 4.36; found C 48.52, H 4.21, N 4.54.

**Ethyl 3-[2-Nitro-4-(trifluoromethyl)phenyl]-2-(propylthio)propanoate (27):** Treatment of **25** (96 mg, 0.33 mmol) with propanethiol, using the procedure described for **26**, gave **27** (55 mg, 45%) as a yellow oil. IR ( $\text{CHCl}_3$ ):  $\tilde{\nu} = 1715 \text{ cm}^{-1}$ .  $^1\text{H}$  NMR:  $\delta = 0.96$  (t,  $J = 7.4 \text{ Hz}$ , 3 H), 1.26 (t,  $J = 7.1 \text{ Hz}$ , 3 H), 1.60 (septet,  $J = 7.3 \text{ Hz}$ , 2 H), 2.64

(dt,  $J = 12.7, 7.7$  Hz, 2 H), 3.39 (dd,  $J = 13.6, 6.7$  Hz, 1 H), 3.52 (dd,  $J = 13.6, 8.4$  Hz, 1 H), 3.65 (dd,  $J = 8.3, 6.7$  Hz, 1 H), 4.15–4.20 (m, 2 H), 7.61 (d,  $J = 8.0$  Hz, 1 H), 7.82 (dd,  $J = 8.0, 1.2$  Hz, 1 H), 8.28 (s, 1 H) ppm.  $^{13}\text{C}$  NMR:  $\delta = 13.7, 14.5, 22.9, 34.3, 35.6, 46.8, 61.2, 122.8$  (q,  $^3J = 3.6$  Hz), 123.2 (q,  $^1J = 273.5$  Hz), 129.7 (q,  $^3J = 3.6$  Hz), 131.4 (q,  $^2J = 34.5$  Hz), 134.9, 137.6, 149.6, 172.1 ppm.  $^{19}\text{F}$  NMR:  $\delta = -63.4$  (s) ppm. HRMS (EI):  $m/z = 365.0896$  (15,  $\text{M}^+$  [ $\text{C}_{15}\text{H}_{18}\text{F}_3\text{NO}_4\text{S}$ ] = 365.0908), 161.0632 {65, [ $\text{C}_7\text{H}_{13}\text{O}_2\text{S}$ ] = 161.0636,  $\text{CH}(\text{SPr})\text{COOEt}$ }.  $\text{C}_{15}\text{H}_{18}\text{F}_3\text{NO}_4\text{S}$  (365.37): calcd. C 49.31, H 4.97, N 3.83; found C 49.52, H 5.21, N 3.64.

**Supporting Information Available:** Energies of all reactants, intermediates, transition states, and products in the gas and solution phases at the B3LYP//HF/6-31+G(d) level (pages S2–S3); gas-phase energies of reactants, intermediates, and transition states at the HF/6-31+G(d) level for models **1**, **6**, **7**, **9**, **11**, **14**, **15**, **16** (S4); partial atomic charges, energy of the electrophile's LUMO, and contributions to the electrophile's LUMO in the gas and solution phases for all models (S5–S6); Cartesian coordinates of all reactants, intermediates, transition states, and products optimized at the HF/6-31+G(d) level in the gas phase (S7–S37).

- [1] For a general review, see: [1a] E. D. Bergmann, D. Ginsburg, R. Pappo, *Org. React.* **1959**, *10*, 179–555. [1b] T. Mukaiyama, S. Kobayashi, *Org. React.* **1994**, *46*, 1–104 (tin enolates in Michael reaction). [1c] R. D. Little, M. R. Masjedizadeh, O. Wallquist, J. I. McLoughlin, *Org. React.* **1995**, *47*, 315–552 (intramolecular Michael reaction). [1d] J. S. Johnson, D. A. Evans, *Acc. Chem. Res.* **2000**, *33*, 325–335 (enantioselective Michael reaction). [1e] J. Christoffers, *Synlett* **2001**, 723–732 (vinylogous Michael reaction).
- [2] S. S. Wong, M. N. Paddon-Row, Y. Li, K. N. Houk, *J. Am. Chem. Soc.* **1990**, *112*, 8679–8686.
- [3] B. E. Thomas IV, P. A. Kollman, *J. Org. Chem.* **1995**, *60*, 8375–8383.
- [4] R. Martínez, H. A. Jiménez-Vázquez, J. Tamariz, *Tetrahedron* **2000**, *56*, 3857–3866.
- [5] S. Okumoto, S. Yamabe, *J. Org. Chem.* **2000**, *65*, 1544–1548.
- [6] K. Hori, S. Higuchi, A. Kamimura, *J. Org. Chem.* **1990**, *55*, 5900–5905.
- [7] L. Pardo, R. Osman, H. Weinstein, J. R. Rabinowitz, *J. Am. Chem. Soc.* **1993**, *115*, 8263–8269.
- [8] R. Janoschek, W. M. F. Fabian, *J. Org. Chem.* **1999**, *64*, 3271–3277.
- [9] C. I. Bayle, F. Grein, *Can. J. Chem.* **1989**, *67*, 2173–2177.
- [10] J. Kona, W. M. F. Fabian, P. Zahradnik, *J. Chem. Soc., Perkin Trans. 2* **2001**, 422–426.
- [11] [11a] B. Deschamps, N. T. Anh, N. J. S. Penne, *Tetrahedron Lett.* **1973**, *14*, 527–530. [11b] J. Durand, N. T. Anh, J. Huet, *Tetrahedron Lett.* **1974**, *15*, 2397–2400.
- [12] I. Fleming, *Frontier Orbitals and Organic Chemical Reactions*, John Wiley & Sons, New York, **1976**.
- [13] I. V. Solodin, A. V. Eremeev, I. I. Chervin, R. G. Kostyanovskii, *Khim. Geterotsikl. Soedin.* **1985**, 1359–1362.
- [14] E. Lewandowska, S. Kinastowski, S. F. Wnuk, *Can. J. Chem.* **2002**, *80*, 192–199.
- [15] [15a] B. M. Trost, G. R. Dake, *J. Am. Chem. Soc.* **1997**, *119*, 7595–7596. [15b] B. Liu, R. Davis, B. Joshi, E. W. Reynolds, *J. Org. Chem.* **2002**, *67*, 4595–4598.
- [16] [16a] S. Miertus, E. Scrocco, J. Tomasi, *Chem. Phys.* **1981**, *55*, 117–129. [16b] J. Tomasi, R. Bonaccorsi, R. Cammi, F. J. O. Valle, *J. Mol. Struct. (THEOCHEM)* **1991**, *234*, 401–424.
- [17] Gaussian 98, Revision A. 9, J. J. Frisch, G. W. Trucks, H. B. Schlegel, G. E. Scuseria, M. A. Robb, J. R. Cheeseman, V. G. Zakrzewski, J. A. Montgomery, R. E. Stratmann, J. C. Burant, S. Dapprich, J. M. Millam, A. D. Daniels, K. N. Kudin, M. C. Strain, O. Farkas, J. Tomasi, V. Barone, M. Cossi, R. Cammi, B. Mennucci, C. Polmelli, C. Adamo, S. Clifford, J. Ochterski, G. A. Petersson, P. Y. Ayala, Q. Cui, K. Morokuma, D. K. Malick, A. D. Rabuck, K. Raghavachar, J. B. Foresman, J. Cioslowski, J. V. Ortiz, B. B. Stefanov, G. Lui, A. Liashenko, P. Piskorz, I. Komaromi, R. Gomperts, R. L. Martin, D. J. Fox, T. Keith, M. A. Al-Laham, C. Y. Peng, A. Nanayakkara, C. Gonzalez, M. Challacombe, P. M. W. Gill, B. G. Johnson, W. Chen, M. W. Wong, J. L. Andres, M. Head-Gordon, E. S. Replogle, J. A. Pople, Gaussian, Inc., Pittsburgh, PA, **1998**.
- [18] M. J. Frisch, A. Frisch, J. B. Foresman, *Gaussian 98 User's Reference, 2nd ed.*; Gaussian, Inc.: Pittsburgh, **1999**, p. 172.
- [19] C. J. Cramer, *Essentials of Computational Chemistry*, Wiley, Chichester, UK, **2002**.
- [20] H. G. Burgi, J. D. Dunitz, L. M. Lehn, G. Wipff, *Tetrahedron* **1974**, *30*, 1563–1572.
- [21] G. S. Hammond, *J. Am. Chem. Soc.* **1955**, *77*, 334–338.
- [22] For  $\alpha$ -addition to **2** and **4**, relaxed potential energy scans in which the  $\text{C}_\text{N}-\text{C}_\alpha$  distance was varied displayed different maxima, depending upon whether the scan was in the forward (decreasing distance) or reverse (increasing distance) direction. The full transition state optimizations for **2** and **4** were initiated with the geometry of the maximum from the forward scan. Selected scans of  $\alpha$ - and  $\beta$ -addition to other compounds did not have this problem with hysteresis.
- [23] C. M. Breneman, K. B. Wiberg, *J. Comp. Chem.* **1990**, *11*, 361–373.

Received August 19, 2003